Appl. Comput. Harmon. Anal. • • • (• • • •) • • •–• • •

Contents lists available at ScienceDirect

Applied and Computational Harmonic Analysis

www.elsevier.com/locate/acha

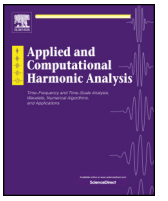

Letter to the Editor

Irregular sampling of band-limited functions on the sphere ☆

Kamen Ivanov [a], Pencho Petrushev [a,b,*]

[a] *Institute of Mathematics and Informatics, Bulgarian Academy of Sciences, 1113 Sofia, Bulgaria*
[b] *Department of Mathematics, University of South Carolina, Columbia, SC 29208, USA*

ARTICLE INFO

Article history:
Received 27 September 2013
Received in revised form 5 May 2014
Accepted 13 May 2014
Available online xxxx
Communicated by W.R. Madych

MSC:
65T99
42C10
33C55
65D15

Keywords:
Spherical harmonics
Irregular sampling
Band-limited functions on the sphere
Needlets
Fast computation

ABSTRACT

An iterative algorithm for stable and accurate reconstruction of band-limited functions from irregular samples on the unit 2-d sphere is developed. Geometric rate of convergence in the uniform norm is achieved. It is shown that a MATLAB realization of this algorithms can effectively recover high degree (≥ 2000) spherical polynomials from their values at sufficiently dense scattered points on the sphere.

1. Introduction

In this article we consider the problem for irregular sampling of high degree spherical polynomials (band-limited functions) on the unit 2-d sphere $\mathbb{S}^2$ in $\mathbb{R}^3$. More explicitly, denoting by Π_N the set of all spherical polynomials of degree N, we focus on the following

Problem 1. Given a finite set Y of irregular sampling points on the sphere $\mathbb{S}^2$ and the values $f(y)$, $y \in Y$, of a spherical polynomial $f \in \Pi_N$ compute to prescribed accuracy ε the values $f(z)$ at the points z of an *arbitrary* set $Z \subset \mathbb{S}^2$.

☆ The first author has been supported by Grant DDVU 02/30 of the Fund for Scientific Research of the Bulgarian Ministry of Education and Science. The second author has been supported by NSF Grant DMS-1211528.

* Corresponding author at: Department of Mathematics, University of South Carolina, Columbia, SC 29208, USA. Fax: +1 803 777 6527.
E-mail addresses: kamen@math.bas.bg (K. Ivanov), pencho@math.sc.edu (P. Petrushev).

http://dx.doi.org/10.1016/j.acha.2014.05.001
1063-5203/

Of course, this problem has a solution only if the density of sampling points is sufficiently high. Our main goal is to devise a fast and stable algorithm for solving Problem 1 with prescribed accuracy measured in the uniform norm, in the case when N is of magnitude 1000 or higher.

Our idea is to split this problem into two:

Problem 2. Given the irregular sampling values $f(y)$, $y \in Y$, of a spherical polynomial $f \in \Pi_N$ compute to prescribed accuracy ε its values $f(\xi)$ at *regular* grid points $\xi \in \mathcal{X} \subset \mathbb{S}^2$.

Problem 3. Given the values $f(\xi)$ of a spherical polynomial $f \in \Pi_N$ at regular grid points $\xi \in \mathcal{X}$ compute to prescribed accuracy ε the values $f(z)$ at the points z of an *arbitrary* set $Z \subset \mathbb{S}^2$.

The notion of a set $\mathcal{X}$ of *regular grid points* needs clarification. In the periodic case, $\mathcal{X}$ would be a set of uniformly distributed points. A set $\mathcal{X} \subset \mathbb{S}^2$ will be deemed regular if the values $f(\xi)$, $\xi \in \mathcal{X}$, of any polynomial $f \in \Pi_N$ allow for fast and accurate evaluation of $f(z)$ at the points z of an arbitrary set $Z \subset \mathbb{S}^2$. Necessarily the cardinality $|\mathcal{X}|$ of $\mathcal{X}$ must be larger than $(N+1)^2$. We shall utilize product-type sets of regular grid points based on 1-d uniformly distributed points and 1-d Gaussian points in spherical coordinates. The notion of a set of regular grid points on $\mathbb{S}^2$ will be further precised in Sections 2 and 3.

Traditionally, to reconstruct a spherical polynomial means to compute its spherical harmonic coefficients, see e.g. [8,10,11]. Unlike the trigonometric case, however, currently there are no satisfactory practical algorithms (like FFT) for fast, stable and accurate evaluation of high degree (≥ 2000) spherical polynomials. (The problem here is with the evaluation of the associated Legendre functions.) This is our motivation for putting forward and utilizing the following principle:

A spherical polynomial $f \in \Pi_N$ is better represented by its values $f(\xi)$ at regular grid points $\xi \in \mathcal{X}$ rather than by its spherical harmonics coefficients.

This article is devoted to the solution of Problem 2. We develop an iterative method based on ideas from [2–5] employing discrete, reproducing Π_N, operators of the form

$$\Phi_N f(x) = \sum_{\xi \in \mathcal{X}} w_\xi \mathcal{K}_N(x \cdot \xi) f(\xi), \tag{1.1}$$

which rely on highly localized kernels (spherical needlets) $\mathcal{K}_N(x \cdot \xi)$, and their truncated versions:

$$\Phi_{N,\delta} f(x) = \sum_{\substack{\xi \in \mathcal{X} \\ \rho(x,\xi) \leq \delta}} w_\xi \mathcal{K}_N(x \cdot \xi) f(\xi). \tag{1.2}$$

Here $x \cdot \xi$ stands for the inner product of $x, \xi \in \mathbb{R}^3$ and $\rho(\cdot, \cdot)$ denotes the geodesic distance on $\mathbb{S}^2$. The rate of convergence of the algorithm is geometric, measured in the uniform norm.

A fast, stable and memory efficient solution of Problem 3 based on operators Φ_N and $\Phi_{N,\delta}$ as above is given in [7].

In this article, we put the emphasis on the computational feasibility and practical realization of the algorithms. Robust MATLAB code realizing our algorithm for solving Problem 2 is developed and examples of effective reconstruction of high degree (≥ 2000) spherical polynomials from irregular sampling values are demonstrated.

The sampling algorithm from this paper can be applied to sampling of band-limited functions or polynomials in various other settings, including the d-dimensional sphere, ball, and simplex with classical weights.

The idea of using spherical needlets for sampling of high degree spherical polynomials is rooted in the highly localized kernels, developed in [13,14], where they are used for the construction of frames on the sphere (termed also needlets).

Please cite this article in press as: K. Ivanov, P. Petrushev, Irregular sampling of band-limited functions on the sphere, Appl. Comput. Harmon. Anal. (2014), http://dx.doi.org/10.1016/j.acha.2014.05.001

There is a considerable body of work on sampling. We find, however, suitable to only exhibit the connections between our sampling algorithm and the relevant algorithms in the literature. As already mentioned our reconstruction algorithm borrows from [2–5]. The main distinction between our approach to sampling and the one in these papers is in our usage of discrete operators as in (1.2) with highly localized kernels and the recovery of the functions at regular grid points.

In [8,10,11] the authors apply a least squares approach to the problem for reconstruction of spherical polynomials from scattered sample values. The proposed algorithm recovers the spherical harmonics coefficients of the polynomials. However, the algorithm relies on the basis transformation from Legendre to Chebyshev polynomials, which creates instability. In a follow up paper [9] this instability was investigated in greater detail. In addition, as it will be explained in Remark 3.4 below, to work properly the algorithm from [8,10,11] requires much denser sets of scattered points on $\mathbb{S}^2$ compared with our algorithm.

The paper is organized as follows. In Section 2 we make the needed preparations for developing our algorithm for reconstruction of spherical polynomials from irregular samples. This algorithm is given in Section 3. A detailed description of the software realization of our sampling algorithm on the sphere along with examples is given in Section 4 and Section 5.

We will denote by c positive constants which may vary at every appearance and by c_1, c_2, c_3 and the alike positive constants which preserve their values throughout the paper. For a finite set E we denote by $|E|$ the number of its elements.

2. Discrete operators reproducing spherical polynomials

The present section lays down some of the ground work that will be needed for developing our sampling algorithm on the sphere. Our goal here is to construct linear operators with highly localized kernels that reproduce spherical polynomials.

2.1. Regular point sets on the sphere

Given $M \in \mathbb{N}$ we say that $\mathcal{X}$ is a set of *M-regular* points on the sphere if the following two conditions are verified:

(1) There exist *non-negative* weights w_ξ, $\xi \in \mathcal{X}$, of a cubature formula with $\mathcal{X}$ as a nodal set which is exact for the polynomials from Π_{M-1}, i.e.

$$\frac{1}{4\pi}\int_{\mathbb{S}^2} f(y)\,d\sigma(y) = \sum_{\xi\in\mathcal{X}} w_\xi f(\xi) \quad \forall f \in \Pi_{M-1}, \tag{2.1}$$

and there exists a companion to $\mathcal{X}$ disjoint partition $\{\mathcal{D}_\xi\}_{\xi\in\mathcal{X}}$ of $\mathbb{S}^2$ ($\mathbb{S}^2 = \cup_{\xi\in\mathcal{X}}\mathcal{D}_\xi$) consisting of measurable sets such that

$$\mathcal{D}_\xi \subset B\big(\xi, c_1 M^{-1}\big) \quad \text{and} \quad w_\xi \le c_2\mu(\mathcal{D}_\xi), \quad \xi \in \mathcal{X}, \tag{2.2}$$

where c_1, $c_2 > 0$ are constants.

(2) The set $\mathcal{X}$ is *structured* in the sense that for every $x \in \mathbb{S}^2$ and $\delta \in (0, \pi]$ one can determine effectively all points in $\bar{B}_\mathcal{X}(x,\delta) = \{\xi \in \mathcal{X} : \rho(x,\xi) \le \delta\}$ using $c_3|\bar{B}_\mathcal{X}(x,\delta)|$ operations, where the constant c_3 is independent of x, δ, M and $|\mathcal{X}|$.

Observe that conditions (2.2) are not quite restrictive and allow us the freedom to choose convenient cubature formulae. The existence of cubature formulae in our setting follows from the general results in

Please cite this article in press as: K. Ivanov, P. Petrushev, Irregular sampling of band-limited functions on the sphere, Appl. Comput. Harmon. Anal. (2014), http://dx.doi.org/10.1016/j.acha.2014.05.001

[12,13]. The overriding requirement for computational efficiency (speed and minimum memory use), however, forces us to utilize product-type grid points whose spherical coordinates are equally distributed or Gaussian.

Examples of regular point sets on the sphere are $\mathcal{X}^{(i)} = \{\xi_{k,\ell}^{(i)} = (\theta_k^{(i)}, \lambda_\ell^{(i)})\}$, $i = 1, 2$, that for given K, $L \geq 1$ are defined by

$$\theta_k^{(1)} = \frac{\pi}{K}k, \quad k = 0, 1, \dots, K; \qquad \lambda_\ell^{(1)} = \frac{2\pi}{L}\ell, \quad \ell = 0, 1, \dots, L-1;$$

and

$$\theta_k^{(2)} = \frac{\pi}{K}k - \frac{\pi}{2K}, \quad k = 1, 2, \dots, K; \qquad \lambda_\ell^{(2)} = \frac{2\pi}{L}\ell, \quad \ell = 0, 1, \dots, L-1.$$

Here in $\mathcal{X}^{(1)}$ we have L coinciding nodes for $k = 0$ (the North Pole) and L such nodes for $k = K$ (the South Pole).

Another example of a regular point set is the set $\mathcal{X}^{(3)}$ generated by the zeros u_k of the K-th degree Legendre polynomial P_K. In this case we define

$$\theta_k^{(3)} = \arccos u_k, \quad k = 1, 2, \dots, K; \qquad \lambda_\ell^{(3)} = \frac{2\pi}{L}\ell, \quad \ell = 0, 1, \dots, L-1.$$

As is well-known each of the cubatures associated with $\mathcal{X}^{(1)}$, $\mathcal{X}^{(2)}$, $\mathcal{X}^{(3)}$ can be represented as a tensor product of a one-dimensional algebraic quadrature in the co-latitude direction θ and a rectangular trigonometric quadrature in the latitude direction (see e.g. [7, Subsection 3.4]). Namely, the weights corresponding to the nodes $\xi_{k,\ell}^{(i)}$ are given by $w_{k,\ell}^{(i)} = v_k^{(i)} L^{-1}$, $i = 1, 2, 3$; $\ell = 0, 1, \dots, L-1$, where

$$\begin{aligned}
v_0^{(1)} &= v_K^{(1)} := \frac{1}{2K(2R+1)}, \\
v_k^{(1)} &:= \frac{1}{K}\left(\frac{1}{2R+1} + 4\sum_{r=1}^{R}\frac{\sin^2 r\theta_k^{(1)}}{4r^2-1}\right), \quad k = 1, \dots, K-1, \ R = \lfloor (K-1)/2 \rfloor; \\
v_k^{(2)} &:= \frac{1}{K}\left(\frac{1}{2R+1} + 4\sum_{r=1}^{R}\frac{\sin^2 r\theta_k^{(2)}}{4r^2-1}\right), \quad k = 1, \dots, K, \ R = \lfloor (K-1)/2 \rfloor; \\
v_k^{(3)} &:= \left(P_K'\left(\cos\theta_k^{(3)}\right)\sin\theta_k^{(3)}\right)^{-2}, \quad k = 1, \dots, K.
\end{aligned}$$

To compute the knots $u_k = \cos\theta_k^{(3)}$ and weights $v_k^{(3)}$ of the Gaussian quadrature we use the MATLAB function `legpts` from `Chebfun` software system by Trefethen et al. [15]. It utilizes a fast and accurate algorithm from Glaser, Liu and Rokhlin [6], which shows very good results for quadratures with up to a million knots.

The relations between K, L and M are given by (see [7, Theorem 3.11])

$$M \leq L, \qquad M \leq \begin{cases} 2\lfloor (K+1)/2 \rfloor, & i = 1, 2; \\ 2K, & i = 3. \end{cases}$$

Under the above restrictions the sets $\mathcal{X}^{(1)}$, $\mathcal{X}^{(2)}$, $\mathcal{X}^{(3)}$ are M-regular [7, Theorems 3.11 and 3.12].

Other regular point sets can be obtained from $\mathcal{X}^{(1)}$, $\mathcal{X}^{(2)}$, or $\mathcal{X}^{(3)}$ by applying rotations or reflections on the sphere. For example, consider the map $T : \mathbb{R}^3 \to \mathbb{R}^3$ given by

$$T(x_1, x_2, x_3) = (x_1, x_3, -x_2).$$

Please cite this article in press as: K. Ivanov, P. Petrushev, Irregular sampling of band-limited functions on the sphere, Appl. Comput. Harmon. Anal. (2014), http://dx.doi.org/10.1016/j.acha.2014.05.001

This is $\pi/2$ rotation about the x_1-axis. The restriction of T on the sphere $T|_{\mathbb{S}^2} : \mathbb{S}^2 \to \mathbb{S}^2$ relates the spherical coordinates (θ, λ) and $(\tilde{\theta}, \tilde{\lambda})$ of a point x and its image $\tilde{x} = T(x)$ by

$$(\sin\tilde{\theta}\cos\tilde{\lambda}, \sin\tilde{\theta}\sin\tilde{\lambda}, \cos\tilde{\theta}) = (\sin\theta\cos\lambda, \cos\theta, -\sin\theta\sin\lambda).$$

From the rotation invariance of Π_N it follows that the sets $T(\mathcal{X}^{(i)})$ and $T^{-1}(X^{(i)})$, $i = 1, 2, 3$, are also regular and induce similar cubatures as $\mathcal{X}^{(i)}$.

All of the above regular point sets have a drawback – their points congregate near the poles (or the respective images of the poles). This will force us later on (see Section 3.2) to treat the points near the poles differently compared to the ones away from the poles.

2.2. Spherical needlets

Very well localized reproducing kernels (father needlets) for high degree spherical polynomials will be the main vehicle in designing our sampling algorithm. The father needlets will be defined via kernels of the form

$$\mathcal{K}_N(u) = \sum_{\nu=0}^{\infty} \varphi\left(\frac{\nu}{N}\right)(2\nu+1)P_\nu(u), \quad u \in [-1, 1], \tag{2.3}$$

where P_ν is the Legendre polynomial of degree ν normalized by $P_\nu(1) = 1$ and φ is a continuous cutoff function satisfying

$$\varphi(t) = 1, \quad t \in [0, 1];\ 0 \le \varphi(t) \le 1,\ t \in [1, 1+\tau];\ \varphi(t) = 0,\ t \ge 1+\tau \tag{2.4}$$

for some fixed $\tau > 0$.

Clearly, the integral operator

$$\breve{\Phi}_N f(x) := \frac{1}{4\pi}\int_{\mathbb{S}^2} \mathcal{K}_N(x \cdot y) f(y)\, d\sigma(y) \tag{2.5}$$

reproduces spherical polynomials of degree N, i.e. $\breve{\Phi}_N f = f$ for $f \in \Pi_N$.

Note that kernels as $\mathcal{K}_N(x \cdot y)$ above have been widely used in Approximation theory and Numerical analysis. For example, see [1] and the references therein.

We next discretize $\breve{\Phi}_N$. For a set of *M-regular* points $\mathcal{X} \subset \mathbb{S}^2$, $M \ge \lceil (2+\tau)N \rceil$, using the weights w_ξ from (2.1) we define the linear operator Φ_N by

$$\Phi_N f(x) = \sum_{\xi \in \mathcal{X}} w_\xi \mathcal{K}_N(x \cdot \xi) f(\xi). \tag{2.6}$$

Clearly, $\Phi_N f = f$ for $f \in \Pi_N$ and $\Phi_N : \ell^\infty(\mathcal{X}) \mapsto \Pi_{N_\tau}$ with

$$N_\tau = \lceil (1+\tau)N \rceil - 1. \tag{2.7}$$

The superb localization of the kernel $\mathcal{K}_N$ implies that most of the terms in (2.6) are very small and this leads us to the idea of introducing the truncated operator

$$\Phi_{N,\delta} f(x) = \sum_{\substack{\xi \in \mathcal{X} \\ \rho(x,\xi) \le \delta}} w_\xi \mathcal{K}_N(x \cdot \xi) f(\xi), \tag{2.8}$$

Please cite this article in press as: K. Ivanov, P. Petrushev, Irregular sampling of band-limited functions on the sphere, Appl. Comput. Harmon. Anal. (2014), http://dx.doi.org/10.1016/j.acha.2014.05.001

where $\delta > 0$ is a small parameter. Observe that the above sum includes only summands corresponding to nodes $\xi \in \mathcal{X}$, which are in the δ-neighborhood of the point x.

We shall also need the rotated by T versions $\tilde{\Phi}_N$, $\tilde{\Phi}_{N,\delta}$ of the operators Φ_N, $\Phi_{N,\delta}$ defined in (2.6) and (2.8) with $\mathcal{X}$ replaced by $T(\mathcal{X})$, i.e.

$$\tilde{\Phi}_N f(x) = \sum_{\xi \in T(\mathcal{X})} \widetilde{w}_\xi \mathcal{K}_N(x \cdot \xi) f(\xi), \quad \tilde{\Phi}_{N,\delta} f(x) = \sum_{\substack{\xi \in T(\mathcal{X}) \\ \rho(x,\xi) \le \delta}} \widetilde{w}_\xi \mathcal{K}_N(x \cdot \xi) f(\xi),$$

where $\widetilde{w}_\xi = w_{T^{-1}(\xi)}$ for $\xi \in T(\mathcal{X})$.

2.3. Localization of spherical needlets

In this subsection we discuss the question of how small δ in (2.8) can be in order that $\Phi_{N,\delta} f$ be a good approximation to $f \in \Pi_N$. The following simple claim gives the first answer (see [7, Theorem 2.4]):

Proposition 2.1. *If*

$$\left|\mathcal{K}_N(\cos\theta)\right| \le \varepsilon \quad \text{for } \delta \le \theta \le \pi, \tag{2.9}$$

then for any function $f : \mathcal{X} \to \mathbb{R}$ we have

$$\|\Phi_N f - \Phi_{N,\delta} f\|_{L_\infty(\mathbb{S}^2)} \le \varepsilon \|f\|_{\ell^\infty(\mathcal{X})}. \tag{2.10}$$

According to [7, Theorem 3.2] for any $\varepsilon > 0$ there exists a cutoff function φ satisfying (2.4) such that (2.9) holds with

$$\delta \le c \frac{\ln(N^2) + \ln(1/\varepsilon) + \ln(1+\tau)}{\tau N}. \tag{2.11}$$

In Proposition 2.1 condition (2.9) can be replaced by

$$\frac{1}{2} \int_{-1}^{\cos\delta} \left|\mathcal{K}_N(u)\right| du = \varepsilon \qquad \left(= \frac{\varepsilon}{2} \int_{-1}^{1} \mathcal{K}_N(u)\, du \right) \tag{2.12}$$

and still have (2.10) as an approximate inequality (see [7, (3.11)]). On account of [7, Theorem 3.6] for any $\varepsilon > 0$ there exists a cutoff function φ obeying (2.4) such that (2.12) holds with

$$\delta \le c \frac{\ln(1/\varepsilon)}{\tau N}. \tag{2.13}$$

Estimate (2.13) is an improvement of (2.11) mainly due to the missing $\ln N$ term in the numerator. One can have $c = 2.5$ in (2.13) when working with cutoff functions φ (satisfying (2.4)) given by

$$\varphi(t) = \kappa^{-1} \int_{(t-1)/\tau}^{1} e^{b\sqrt{v(1-v)}}\, dv, \qquad \kappa = \int_0^1 e^{b\sqrt{v(1-v)}}\, dv, \quad b > 0, \tag{2.14}$$

for t in $[1, 1+\tau]$. In (2.14) b is a parameter, which for $4 < \log_{10}(1/\varepsilon) < 11$ and $\tau \ge 1$ is given by

$$b = 4.8 \log_{10}(1/\varepsilon) + 3.4 - 0.2 \min\{\tau, 3\}. \tag{2.15}$$

For more details, see [7].

Please cite this article in press as: K. Ivanov, P. Petrushev, Irregular sampling of band-limited functions on the sphere, Appl. Comput. Harmon. Anal. (2014), http://dx.doi.org/10.1016/j.acha.2014.05.001

3. Sampling of band-limited functions on the sphere: algorithm

We begin by formulating somewhat more precisely the problem we want to solve.

Problem 2. Given a set of sampling points $Y \subset \mathbb{S}^2$ and the values $f(y)$ of a polynomial $f \in \Pi_N$ at the points $y \in Y$ compute to prescribed accuracy ε measured in the uniform norm the values $f(\xi)$ of the polynomial f at the $\lceil (2+\tau)N \rceil$-*regular* points $\xi \in \mathcal{X} \subset \mathbb{S}^2$. Here $\tau > 0$ is the needlet parameter from (2.4).

The main input in Problem 2 are the set Y and the degree N. We are free to choose the *regular* set $\mathcal{X}$ because the solution of Problem 2 for a particular regular set $\mathcal{X}$ combined with the solution of Problem 3 would imply a solution of Problem 1 and hence of Problem 2 for an arbitrary regular set $\mathcal{X}$. Thus, the regular sets $\mathcal{X} = \mathcal{X}^{(i)}$, $i = 1, 2, 3$, from Section 2.1 can be utilized in solving Problem 2 as the respective cubature weights are known in advance.

A needlet based fast and stable algorithm for solving Problem 3 is developed in [7]. An *exact solution* of Problem 3 is given by $f(z) = \Phi_N f(z)$ and an *approximate solution* by $f(z) \approx \Phi_{N,\delta} f(z)$, where Φ_N and $\Phi_{N,\delta}$ are defined in (2.6) and (2.8).

3.1. Exact solution of Problem 2

Given a finite set of sampling points $Y \subset \mathbb{S}^2$ let $\mathcal{A} = \{A_y\}_{y \in Y}$ be a disjoint partition of $\mathbb{S}^2$ consisting of measurable sets A_y, such that $y \in A_y$.

In particular, $\{A_y\}$ can be the Voronoi tessellation of $\mathbb{S}^2$ induced by Y, where the common points from the boundaries of several cells are attached to exactly one of the cells. Another meaningful example are the HEALPix centers Y with the pixels collected in $\{A_y\}$.

The following notation will be useful: For any $x \in \mathbb{S}^2$ we denote by y_x the point in Y such that $x \in A_{y_x}$. Consider the extension operator

$$\mathcal{E}_{\mathcal{A}} g(x) := \sum_{y \in Y} g(y) \mathbb{1}_{A_y}(x) = g(y_x) \tag{3.1}$$

defined for any function $g : Y \to \mathbb{R}$, where $\mathbb{1}_{A_y}$ is the characteristic function of A_y. Obviously $\|\mathcal{E}_{\mathcal{A}}\| = 1$ (all operator norms are $\infty \mapsto \infty$ norms). Denote

$$d(\mathcal{A}) := \max_{y \in Y} \sup_{x \in A_y} \rho(x, y). \tag{3.2}$$

Theorem 3.1. *Assume that the bounded linear operator $\Phi : \ell^\infty(\mathcal{X}) \to \Pi_{N_\tau}$ preserves the polynomials from Π_N. Let*

$$q := d(\mathcal{A}) N_\tau \|\Phi\| < 1. \tag{3.3}$$

Set $\mathcal{R} = (\mathcal{I} - \mathcal{E}_{\mathcal{A}})\Phi$, where $\mathcal{I}$ denotes the identity. Then for any $f \in \Pi_N$

$$f = \sum_{k=0}^{\infty} \mathcal{R}^k (\mathcal{E}_{\mathcal{A}} f) \tag{3.4}$$

with the series converging uniformly and

$$\left\| f - \sum_{k=0}^{n-1} \mathcal{R}^k (\mathcal{E}_{\mathcal{A}} f) \right\|_\infty \le q^n \|f\|_\infty, \quad n \ge 1. \tag{3.5}$$

Please cite this article in press as: K. Ivanov, P. Petrushev, Irregular sampling of band-limited functions on the sphere, Appl. Comput. Harmon. Anal. (2014), http://dx.doi.org/10.1016/j.acha.2014.05.001

Proof. For $f \in \Pi_N$ and $k \geq 0$ we use that $\Phi f = f$ to write

$$\mathcal{R}^k f - \mathcal{R}^{k+1} f = \mathcal{R}^k\big(f - (\mathcal{I} - \mathcal{E}_{\mathcal{A}})\Phi f\big) = \mathcal{R}^k(f - f + \mathcal{E}_{\mathcal{A}} f) = \mathcal{R}^k(\mathcal{E}_{\mathcal{A}} f). \tag{3.6}$$

Hence

$$f - \sum_{k=0}^{n-1} \mathcal{R}^k(\mathcal{E}_{\mathcal{A}} f) = \mathcal{R}^n f, \quad \forall f \in \Pi_N. \tag{3.7}$$

We now estimate $\|\mathcal{R}\|$. Clearly

$$\mathcal{R}g(x) = \Phi g(x) - \mathcal{E}_{\mathcal{A}}\Phi g(x) = \Phi g(x) - \Phi g(y_x) \quad \text{for } g \in L^\infty\big(\mathbb{S}^2\big),\ x \in \mathbb{S}^2.$$

The restriction of Φg to the big circle connecting x and y_x is a trigonometric polynomial of degree N_τ and, therefore, the mean-value theorem and the Bernstein inequality yield

$$\big|\mathcal{R}g(x)\big| \leq \rho(x, y_x) N_\tau \|\Phi g\|_\infty \leq d(\mathcal{A}) N_\tau \|\Phi\| \|g\|_\infty.$$

Hence

$$\|\mathcal{R}\| \leq d(\mathcal{A}) N_\tau \|\Phi\|. \tag{3.8}$$

Now (3.8) and (3.3) give $\|\mathcal{R}\| \leq q$, which implies the uniform convergence of the series in (3.4). The last inequality coupled with (3.7) implies (3.5), yielding (3.4). □

Theorem 3.1 provides an exact reconstruction algorithm for $f \in \Pi_N$. Indeed, pick a $(2+\tau)N-$*regular* point set $\mathcal{X} \subset \mathbb{S}^2$ and set $\Phi := \Phi_N$ with Φ_N being the operator from (2.6). Denote briefly $g_k = \mathcal{R}^k(\mathcal{E}_{\mathcal{A}} f)$. Then Theorem 3.1 implies

$$f(\xi) = \sum_{k=0}^{\infty} g_k(\xi), \quad \xi \in \mathcal{X}, \tag{3.9}$$

which solves Problem 2, and the solution $f(z) = \Phi_N f(z)$ of Problem 3 gives exact reconstruction of f at every $z \in Z \subset \mathbb{S}^2$. Observe that the values $g_k(\xi)$, $\xi \in \mathcal{X}$, can be recursively computed by $g_0(\xi) = f(y_\xi)$ and

$$g_{k+1}(\xi) = \mathcal{R}g_k(\xi) = \Phi_N g_k(\xi) - \Phi_N g_k(y_\xi). \tag{3.10}$$

Note that the evaluation of $\Phi_N g(x)$ by (2.6) uses only the values $g(\xi)$ for $\xi \in \mathcal{X}$.

Of course, for practical purposes we truncate the series in (3.9) to obtain the approximation

$$f(\xi) \approx \sum_{k=0}^{n-1} g_k(\xi),$$

where n is determined by the target accuracy via (3.5).

The complexity of this algorithm is as follows. To determine the y_ξ's one needs $O(|\mathcal{X}| + |Y|)$ operations using that $\mathcal{X}$ is *structured*. Every step in (3.10) requires $O(|\mathcal{X}|^2)$ operations if $\mathcal{K}_N(u)$ can be evaluated with $O(1)$ operations within the machine precision. Thus, the algorithm evaluates $f(\xi)$, $\xi \in \mathcal{X}$, with accuracy ε using $O(|\mathcal{X}|^2 \ln(1/\varepsilon)/\ln(1/q) + |Y|)$ operations.

Please cite this article in press as: K. Ivanov, P. Petrushev, Irregular sampling of band-limited functions on the sphere, Appl. Comput. Harmon. Anal. (2014), http://dx.doi.org/10.1016/j.acha.2014.05.001

3.2. Approximate solution of Problem 2

As already mentioned the regular point sets from Section 2.1 have the deficiency that the points in each of them concentrate around the poles or the images of the poles via some rotation. This drawback along with the fact that the value of $\Phi_N f(x)$ is obtained by $O(|\mathcal{X}|)$ operations makes the sampling algorithm from Section 3.1 impractical. To overcome the second deficiency we shall use the truncated version $\Phi_{N,\delta}$ of the operator Φ_N defined in (2.8), and to remedy the first deficiency we shall utilize the rotated version $\tilde{\Phi}_{N,\delta}$ of $\Phi_{N,\delta}$ for the regions around the poles. In this way we will decrease substantially the algorithm's computational cost outlined at the end of Subsection 3.1.

To realize these ideas we first introduce some notation. Given $N \in \mathbb{N}$ and $\varepsilon > 0$ (to be determined) we assume that $\mathcal{X} \subset \mathbb{S}^2$ is one of the M-regular set points $\mathcal{X}^{(1)}$, $\mathcal{X}^{(2)}$, or $\mathcal{X}^{(3)}$ from Section 2.1 with $M := \lceil (2+\tau)N \rceil$. In fact, to us the best choice is $\mathcal{X} := \mathcal{X}^{(3)}$.

Let $\delta > 0$ be a constant such that (2.9) holds and let $\Phi_{N,\delta}$ be the operator defined in (2.8). We subdivide $\mathbb{S}^2$ into two: The equatorial area (belt) $\mathcal{U}_1$ and its compliment (the polar regions) $\mathcal{U}_2$, defined in spherical coordinates by

$$\mathcal{U}_1 := \big\{x \in \mathbb{S}^2 : \pi/4 \le \theta \le 3\pi/4\big\}, \qquad \mathcal{U}_2 := \mathbb{S}^2 \setminus \mathcal{U}_1. \tag{3.11}$$

We also introduce the following sets of nodes on $\mathbb{S}^2$:

$$\begin{aligned} \mathcal{X}_1 &:= \mathcal{X} \cap \{\pi/4 - \delta_0 \le \theta \le 3\pi/4 + \delta_0\}, \\ \mathcal{X}_2 &:= T(\mathcal{X}) \cap \big(\{0 \le \theta \le \pi/4 + \delta_0\} \cup \{3\pi/4 - \delta_0 \le \theta \le \pi\}\big), \\ \mathcal{X}_0 &:= \mathcal{X}_1 \cup \mathcal{X}_2, \end{aligned} \tag{3.12}$$

where $\delta_0 := \delta + d(\mathcal{A})$. We assume $\delta_0 < \pi/4$.

We now introduce the linear operator

$$\mathcal{R}g(x) := (\mathcal{I} - \mathcal{E}_{\mathcal{A}})\Phi_{N,\delta} g(x) \cdot \mathbb{1}_{\mathcal{U}_1}(x) + (\mathcal{I} - \mathcal{E}_{\mathcal{A}})\tilde{\Phi}_{N,\delta} g(x) \cdot \mathbb{1}_{\mathcal{U}_2}(x). \tag{3.13}$$

The above operator only uses the values of g at the points of $\mathcal{X}_0$. Indeed, if $x \in \mathcal{U}_1$ then $\mathcal{E}_{\mathcal{A}}\Phi_{N,\delta} g(x) = \Phi_{N,\delta} g(y_x)$ uses the values $g(\xi)$ for $\xi \in \mathcal{X}$ and $\rho(y_x, \xi) \le \delta$, hence $\rho(x, \xi) \le \delta + d(\mathcal{A})$, i.e. $\xi \in \mathcal{X}_1$. Let us point out that for these x the value of $\Phi_{N,\delta} g$ at y_x is determined by the values of g at $\mathcal{X}_1$ even in the case when y_x itself belongs to $\mathcal{U}_2$. Similar considerations holds for $x \in \mathcal{U}_2$.

Our algorithm for approximate solution of Problem 2 is contained in the following

Theorem 3.2. *Assume that (2.9) or (2.12) holds for some $\varepsilon > 0$ and $0 < \delta < \pi$. Using the notation from above assume also that*

$$q := d(\mathcal{A}) N_\tau \|\Phi_N\| + 2\varepsilon < 1. \tag{3.14}$$

Then for any $f : Y \to \mathbb{R}$ the series $\sum_{k=0}^{\infty} \mathcal{R}^k(\mathcal{E}_{\mathcal{A}} f)$ converges uniformly and for any $f \in \Pi_N$

$$\left\| f - \sum_{k=0}^{n-1} \mathcal{R}^k(\mathcal{E}_{\mathcal{A}} f) \right\|_\infty \le \left(q^n + \frac{2\varepsilon}{1-q} \right) \|f\|_\infty. \tag{3.15}$$

Proof. We first estimate the norm of the operator $\mathcal{R}$. By (3.13) we have for any function $g : Y \mapsto \mathbb{R}$ and $x \in \mathcal{U}_1$

Please cite this article in press as: K. Ivanov, P. Petrushev, Irregular sampling of band-limited functions on the sphere, Appl. Comput. Harmon. Anal. (2014), http://dx.doi.org/10.1016/j.acha.2014.05.001

$$\begin{aligned}\mathcal{R}g(x) &= \Phi_{N,\delta}g(x) - \Phi_{N,\delta}g(y_x)\\ &= \Phi_N g(x) - \Phi_N g(y_x) + (\Phi_{N,\delta} - \Phi_N)g(x) - (\Phi_{N,\delta} - \Phi_N)g(y_x).\end{aligned}$$

Now just as in the proof of Theorem 3.1 we get

$$\big|\Phi_N g(x) - \Phi_N g(y_x)\big| \le \rho(x, y_x)N_\tau\|\Phi_N\|\|g\|_\infty \le d(\mathcal{A})N_\tau\|\Phi_N\|\|g\|_\infty$$

and by Proposition 2.1

$$\big|(\Phi_{N,\delta} - \Phi_N)g(x)\big| \le \varepsilon\|g\|_\infty, \qquad \big|(\Phi_{N,\delta} - \Phi_N)g(y_x)\big| \le \varepsilon\|g\|_\infty.$$

Putting the above together we arrive at

$$\big|\mathcal{R}g(x)\big| \le \big(d(\mathcal{A})N_\tau\|\Phi_N\| + 2\varepsilon\big)\|g\|_\infty.$$

Exactly in the same way, using $\tilde{\Phi}_{N,\delta}$, $\tilde{\Phi}_N$ instead of $\Phi_{N,\delta}$, Φ_N we obtain the same estimate for $x \in \mathcal{U}_2$. Therefore,

$$\|\mathcal{R}\| \le d(\mathcal{A})N_\tau\|\Phi_N\| + 2\varepsilon = q. \tag{3.16}$$

The uniform convergence of $\sum_{k=0}^\infty \mathcal{R}^k(\mathcal{E}_\mathcal{A}f)$ follows from (3.16) and (3.14).

Let $f \in \Pi_N$. Clearly,

$$\mathcal{R}^k f - \mathcal{R}^{k+1}f = \mathcal{R}^k(f - \mathcal{R}f) = \mathcal{R}^k(\mathcal{E}_\mathcal{A}f) + \mathcal{R}^k(f - \mathcal{E}_\mathcal{A}f - \mathcal{R}f), \quad k \ge 0,$$

and iterating this identity we obtain

$$f - \sum_{k=0}^{n-1}\mathcal{R}^k(\mathcal{E}_\mathcal{A}f) = \mathcal{R}^n f + \sum_{k=0}^{n-1}\mathcal{R}^k(f - \mathcal{E}_\mathcal{A}f - \mathcal{R}f). \tag{3.17}$$

By the definition of $\mathcal{R}$ in (3.13) we have for $x \in \mathbb{S}^2$

$$\begin{aligned}f(x) - \mathcal{E}_\mathcal{A}f(x) - \mathcal{R}f(x) = f(x) - f(y_x) &- \big(\Phi_{N,\delta}f(x) - \Phi_{N,\delta}f(y_x)\big)\cdot \mathbb{1}_{\mathcal{U}_1}(x)\\ &- \big(\tilde{\Phi}_{N,\delta}f(x) - \tilde{\Phi}_{N,\delta}f(y_x)\big)\cdot \mathbb{1}_{\mathcal{U}_2}(x)\end{aligned}$$

and using the fact that $\Phi_N f = f$ and $\tilde{\Phi}_N f = f$ we infer

$$\begin{aligned}f(x) - \mathcal{E}_\mathcal{A}f(x) - \mathcal{R}f(x) = &\big[(\Phi_N - \Phi_{N,\delta})f(x) - (\Phi_N - \Phi_{N,\delta})f(y_x)\big]\cdot \mathbb{1}_{\mathcal{U}_1}(x)\\ &+ \big[(\tilde{\Phi}_N - \tilde{\Phi}_{N,\delta})f(x) - (\tilde{\Phi}_N - \tilde{\Phi}_{N,\delta})f(y_x)\big]\cdot \mathbb{1}_{\mathcal{U}_1}(x),\end{aligned}$$

which can be written in the form

$$f - \mathcal{E}_\mathcal{A}f - \mathcal{R}f = (\mathcal{I} - \mathcal{E}_\mathcal{A})(\Phi_N - \Phi_{N,\delta})f\cdot \mathbb{1}_{\mathcal{U}_1} + (\mathcal{I} - \mathcal{E}_\mathcal{A})(\tilde{\Phi}_N - \tilde{\Phi}_{N,\delta})f\cdot \mathbb{1}_{\mathcal{U}_2}.$$

We now use (2.9)–(2.10) to obtain

$$\|f - \mathcal{E}_\mathcal{A}f - \mathcal{R}f\|_\infty \le 2\varepsilon\|f\|_\infty. \tag{3.18}$$

Combining this with (3.17) and (3.16) yields (3.15). □

Please cite this article in press as: K. Ivanov, P. Petrushev, Irregular sampling of band-limited functions on the sphere, Appl. Comput. Harmon. Anal. (2014), http://dx.doi.org/10.1016/j.acha.2014.05.001

We next explain how the sampling (reconstruction) algorithm based on Theorem 3.2 works. We are given the values $f(y)$, $y \in Y$, of a band-limited function $f \in \Pi_N$. We only need to compute the values $f(\xi)$ at the points $\xi \in \mathcal{X}_0 = \mathcal{X}_1 \cup \mathcal{X}_2$. Then the algorithm for solving Problem 3 enables us to compute the values $f(z)$ at the points $z \in Z$ for an arbitrary set $Z \subset \mathbb{S}^2$.

Denote briefly $g_k := \mathcal{R}^k(\mathcal{E}_\mathcal{A} f)$ with $\mathcal{R}$ defined in (3.13) and $\mathcal{E}_\mathcal{A}$ from (3.1). The values $f(\xi)$ are approximated by

$$f(\xi) \approx \sum_{k=0}^{n-1} g_k(\xi), \quad \xi \in \mathcal{X}_0. \tag{3.19}$$

The gist of our method is that the values $g_k(\xi)$, $\xi \in \mathcal{X}_0$, can be computed recursively. More explicitly, we start from $g_0(\xi) = \mathcal{E}_\mathcal{A} f(\xi) = f(y_\xi)$, $\xi \in \mathcal{X}_0$, and for $k = 0, 1, \dots, n-2$,

$$g_{k+1}(\xi) = \mathcal{R} g_k(\xi) = \Phi_{N,\delta} g_k(\xi) - \Phi_{N,\delta} g_k(y_\xi) \quad \text{if } \xi \in \mathcal{X}_0 \cap \mathcal{U}_1 \tag{3.20}$$

and

$$g_{k+1}(\xi) = \mathcal{R} g_k(\xi) = \tilde{\Phi}_{N,\delta} g_k(\xi) - \tilde{\Phi}_{N,\delta} g_k(y_\xi) \quad \text{if } \xi \in \mathcal{X}_0 \cap \mathcal{U}_2. \tag{3.21}$$

Observe that identities (3.20)–(3.21) are in fact local – the evaluation of $g_{k+1}(\xi)$ involves only the values $g_k(\eta)$ for η satisfying $\rho(\eta, \xi) \le \delta + d(\mathcal{A})$. Therefore, the evaluation of $g_{k+1}(\xi)$ for $\xi \in \mathcal{X}_0 \cap \mathcal{U}_1$ involves only points $\eta \in \mathcal{X}_1$ and the evaluation of $g_{k+1}(\xi)$ for $\xi \in \mathcal{X}_0 \cap \mathcal{U}_2$ involves only points $\eta \in \mathcal{X}_2$.

Remark 3.1. The series in Theorem 3.2 converges to a function $g \in L^\infty$ which is in general different from the polynomial f but satisfies $\|f - g\|_\infty \le \frac{2\varepsilon}{1-q} \|f\|_\infty$.

Remark 3.2. The "remainder" operators $\mathcal{R}$ in Theorem 3.1 can be replaced by $\mathcal{R}_\star = \Phi(\mathcal{I} - \mathcal{E}_\mathcal{A})$. Then Theorem 3.1 remain valid with (3.5) replaced by

$$\left\| f - \sum_{k=0}^{n-1} \mathcal{R}_\star^k (\Phi \mathcal{E}_\mathcal{A} f) \right\|_\infty \le q^n \|\Phi\| \|f\|_\infty.$$

The proof is carried out along the lines of the proof of Theorem 3.1 using the identity $\mathcal{R}_\star^k \Phi = \Phi \mathcal{R}^k$. The advantage of this representation is that we approximate f by polynomials (because the partial sums of the series belong to Π_{N_τ}) and the price we pay is that the error estimate is worsen by the factor $\|\Phi\| > 1$.

A similar observation applies to Theorem 3.2, where we can replace $\mathcal{R}$ by $\mathcal{R}_\star$ defined by

$$\mathcal{R}_\star g(x) := \Phi_{N,\delta}(\mathcal{I} - \mathcal{E}_\mathcal{A}) g(x) \cdot \mathbb{1}_{\mathcal{U}_1}(x) + \tilde{\Phi}_{N,\delta}(\mathcal{I} - \mathcal{E}_\mathcal{A}) g(x) \cdot \mathbb{1}_{\mathcal{U}_2}(x)$$

and (3.15) by

$$\left\| f - \sum_{k=0}^{n-1} \mathcal{R}_\star^k (\Phi_{N,\delta} \mathcal{E}_\mathcal{A} f) \right\|_\infty \le \left(q^n + \frac{2\varepsilon}{1-q} \right) \|\Phi_{N,\delta}\| \|f\|_\infty.$$

Remark 3.3. Note that the smaller q the faster the convergence in (3.4) or in (3.15). Turning our attention to (3.3) or (3.14) we observe that the smallest $d(\mathcal{A})$ is realized whenever $\mathcal{A}$ is the Voronoi tessellation of $\mathbb{S}^2$ induced by Y. Instead of (3.1) one can use other extension operators, e.g. local interpolation.

Please cite this article in press as: K. Ivanov, P. Petrushev, Irregular sampling of band-limited functions on the sphere, Appl. Comput. Harmon. Anal. (2014), http://dx.doi.org/10.1016/j.acha.2014.05.001

Remark 3.4. The norm $\|\Phi_N\|$ plays an essential role in conditions (3.3) and (3.14). This norm has been computed numerically for various values of τ and ε and the results are displayed in Table 6 in Subsection 5.2. For example, if $\tau = 1$ and $\varepsilon = 10^{-5}$, then $\|\Phi_N\| \approx 4.2324$, which implies that the condition $d(\mathcal{A})N < 1/9$ is sufficient for successful reconstruction of spherical polynomials of degree N with relative error $\varepsilon = 10^{-5}$ (or smaller error if δ is increased). For comparison, the similar sufficient condition in [8, Theorem 1] in our notations reads $d(\mathcal{A})N < 1/308$. Therefore, our condition on the sampling set Y is a lot more relaxed than the condition given in [8].

4. Approximate reconstruction algorithm

Assume in Problem 2 we would like to find the approximate values $F(\xi)$ to the unknown values $f(\xi)$, $\xi \in \mathcal{X}_0$, with absolute error ε_0, i.e. $|F(\xi) - f(\xi)| \le \varepsilon_0$. We determine the relative error $\varepsilon_1 = \varepsilon_0/\|f\|_{\ell^\infty(Y)}$ and split it into two parts $\varepsilon_1 = \varepsilon_2 + 2\varepsilon/(1-q)$, where ε_2 will be the iteration accuracy and ε – the needlet accuracy.

Here we describe our *algorithm for approximate reconstruction*. If we consider Problem 2 as a step in the solution of Problem 1, then we are free to chose the regular set $\mathcal{X}_0$ from (3.12) in Subsection 3.2. This case is described below. In the case of fixed $\mathcal{X}_0$ in Problem 2 step (1) from the *Pre-computation* part has to be moved to the *Input* part.

Input:

(1) Values $f(y)$, $y \in Y$, at an irregular sampling set Y.
(2) Degree N of f, the cutoff parameter τ, the target relative accuracy ε_1, the iteration accuracy ε_2 and the needlet accuracy ε.

Pre-computation:

(1) Compute the number of knots K, L so that the cubature be exact for polynomials of degree $M-1$ with $M = \lceil (2+\tau)N \rceil$.
(2) Compute the knots and weights of the one-dimensional quadratures.
(3) Compute the nodes of a regular set $\mathcal{X} = \mathcal{X}^{(3)}$ (see Subsection 2.1).
(4) Compute the weights w_ξ of the cubature (2.1) as tensor product of the one-dimensional quadratures weights.
(5) For every $\xi \in \mathcal{X} \cup T(\mathcal{X})$ find the closest point y_ξ in Y.
(6) Compute δ for the given N, ε, τ and a cutoff function φ from (2.14)–(2.15).
(7) Compute the values $\varphi(k/N)$ for the given N, ε, τ and φ from (2.14)–(2.15).
(8) Compute $\mathcal{K}_N(\cos t_r^*)$, $r = -s, -s+1, \dots, R+s$ with downward Clenshaw recurrence (see [7, Subsection 3.3]).
(9) Compute $d = \max_{\xi \in \mathcal{X}} \rho(\xi \cdot y_\xi)$ and form the sets $\mathcal{X}_i$, $i = 0, 1, 2$, with parameter $\delta_0 = \delta + d$ (see (3.12)).
(10) Compute the matrices:
$V^{(1)} = \{v_{\xi,\eta}^{(1)} : \xi \in \mathcal{X}_1 \cap \mathcal{U}_1, \eta \in \mathcal{X}\}$, $V^{(2)} = \{v_{\xi,\eta}^{(2)} : \xi \in \mathcal{X}_2 \cap \mathcal{U}_2, \eta \in T(\mathcal{X})\}$,
$V^{(3)} = \{v_{\xi,\eta}^{(3)} : \xi \in \mathcal{X}_1 \cap \mathcal{U}_2, \eta \in T(\mathcal{X})\}$, $V^{(4)} = \{v_{\xi,\eta}^{(4)} : \xi \in \mathcal{X}_2 \cap \mathcal{U}_1, \eta \in \mathcal{X}\}$, defined by

$$\begin{aligned} v_{\xi,\eta}^{(j)} &= w_\eta \big(\widetilde{\mathcal{K}}_N(\xi \cdot \eta) - \widetilde{\mathcal{K}}_N(y_\xi \cdot \eta)\big), \quad j = 1, 4, \\ v_{\xi,\eta}^{(j)} &= \widetilde{w}_\eta \big(\widetilde{\mathcal{K}}_N(\xi \cdot \eta) - \widetilde{\mathcal{K}}_N(y_\xi \cdot \eta)\big), \quad j = 2, 3, \end{aligned} \tag{4.1}$$

where $\widetilde{\mathcal{K}}_N(t) = \mathcal{K}_N(t)$ for $t \ge \cos\delta$ and $\widetilde{\mathcal{K}}_N(t) = 0$ for $t < \cos\delta$.

Please cite this article in press as: K. Ivanov, P. Petrushev, Irregular sampling of band-limited functions on the sphere, Appl. Comput. Harmon. Anal. (2014), http://dx.doi.org/10.1016/j.acha.2014.05.001

Iterations:

(1) Initial values: $g_0(\xi) = f(y_\xi), F(\xi) = g_0(\xi), \xi \in \mathcal{X}_0$.
(2) Iteration steps: For $k = 0, 1, \dots$ do
(a)

$$g_{k+1}(\xi) = \sum_{\eta \in \mathcal{X}_1} v^{(1)}_{\xi,\eta} g_k(\eta), \quad \xi \in \mathcal{X}_1 \cap \mathcal{U}_1; \tag{4.2}$$

(b)

$$g_{k+1}(\xi) = \sum_{\eta \in \mathcal{X}_2} v^{(2)}_{\xi,\eta} g_k(\eta), \quad \xi \in \mathcal{X}_2 \cap \mathcal{U}_2; \tag{4.3}$$

(c)

$$g_{k+1}(\xi) = \sum_{\eta \in \mathcal{X}_2} v^{(3)}_{\xi,\eta} g_k(\eta), \quad \xi \in \mathcal{X}_1 \cap \mathcal{U}_2; \tag{4.4}$$

(d)

$$g_{k+1}(\xi) = \sum_{\eta \in \mathcal{X}_1} v^{(4)}_{\xi,\eta} g_k(\eta), \quad \xi \in \mathcal{X}_2 \cap \mathcal{U}_1; \tag{4.5}$$

(e) $F(\xi) = F(\xi) + g_{k+1}(\xi), \xi \in \mathcal{X}_0$;
(3) Stopping criterion: $\|g_{k+1}\| \le \varepsilon_2 \|g_0\|$.

Output: The approximate values $F(\xi)$ of $f(\xi)$ at all points $\xi \in \mathcal{X}_0$.

The only condition which has to be met for the work of the algorithm is (3.14). Under this condition the algorithm has geometric convergence and we have

Proposition 4.1. *Under the assumption of Theorem 3.2 the relative error of the algorithm output is given by*

$$\frac{\|F - f\|_{\ell^\infty(\mathcal{X}_0)}}{\|f\|_{\ell^\infty(Y)}} < \varepsilon_2 + \frac{2\varepsilon}{1-q} = \varepsilon_1, \tag{4.6}$$

$$\max\big\{\|\Phi_{N,\delta} F - f\|_{\ell^\infty(Y \cap \mathcal{U}_1)}, \|\tilde{\Phi}_{N,\delta} F - f\|_{\ell^\infty(Y \cap \mathcal{U}_2)}\big\} < \varepsilon_1 \|\Phi_{N,\delta}\| \|f\|_{\ell^\infty(Y)}. \tag{4.7}$$

Proof. Inequality (4.6) follows from (3.17), (3.16), (3.18) and the Stopping criterion of the *Iterations* part. Inequality (4.7) follows by the same argument if we use the operator $\mathcal{R}_\star$ from Remark 4.2 instead of $\mathcal{R}$. □

Inequality (4.6) shows that the prescribed accuracy is achieved by the algorithm, while (4.7) give us a tool to verify whether the computed values $F(\xi)$, $\xi \in \mathcal{X}_0$, reconstruct the spherical polynomial f, known by its values at the scattered points $y \in Y$.

Complexity of the algorithm. We determine the complexity for the best choice of K and L in step (1), which means $K = O(N)$, $L = O(N)$. Steps (1), (2), (3), (4), (6), (7), and (8) are analyzed in [7, Subsection 3.7]. In view of the structure condition for regular points in Subsection 2.1 step (5) requires $O(N^2 + |Y|)$ operations. The complexity of step (9) is $O(N^2)$.

Step (10) is the most demanding one on both memory and number of operations (i.e. speed) in the whole algorithm. The "matrices of influence" $V^{(j)}$, $j = 1, 2, 3, 4$, express the relative distances between the

Please cite this article in press as: K. Ivanov, P. Petrushev, Irregular sampling of band-limited functions on the sphere, Appl. Comput. Harmon. Anal. (2014), http://dx.doi.org/10.1016/j.acha.2014.05.001

elements of the two sets $\mathcal{X}_0$ and Y. Their size is huge: $V^{(1)}$ and $V^{(2)}$ have $O(N^4)$ elements and $V^{(3)}$ and $V^{(4)}$ have $O(N^4\delta_0)$ elements. If one wants to work with the whole "matrices of influence" then polynomial degrees exceeding 200 will be practically prohibitive. For comparison, for degree 1000 we work with a regular set $\mathcal{X}_0$ with close to 6 000 000 points and the nodal sets $\mathcal{X} = \mathcal{X}^{(3)}$ and $T(\mathcal{X})$ have 8 000 000 points each. This makes a total of 4.8×10^{13} elements in the "matrices of influence" and only the storage of such amount of data on a "hard disk" as 8 bytes numbers will require 350 TB of memory!

Using the superb localization of the father needlet kernel $\mathcal{K}_N(x \cdot \xi)$ we make the "matrices of influence" sparse by setting $\widetilde{\mathcal{K}}_N(t) = 0$ for $t < \cos\delta$ in (4.1). Thus, the total number of non-zero elements in these matrices is $O(N^2\bar{n}) = O(N^4\delta^2) = O(N^2 \ln^2(1/\varepsilon))$, where $\bar{n}$ is the average number per point ξ of non-zero elements in (4.1). Several values of $\bar{n}$ are given in Table 1 below. For $\tau = 2$ they range from 267 for $\varepsilon = 10^{-5}$ to 1150 for $\varepsilon = 10^{-11}$. Other important parameters of the problem as memory requirements and time of execution are also given in Subsection 5.1. In sum, step (10) requires $O(N^2 \ln^2(1/\varepsilon))$ operations but the O constant is quite large.

Every step in the *Iterations* part performs a matrix-times-vector multiplication, where every non-zero element of the "matrices of influence" is used once. This means $O(N^2 \ln^2(1/\varepsilon))$ operations. The number of iterations is $\ln(1/\varepsilon_2)/\ln(1/q)$. Hence the choice $\varepsilon_2 = \varepsilon_1/3$ and $\varepsilon = (1-q)\varepsilon_1/3$ will give $O(N^2 \ln^3(1/\varepsilon_1))$ for the complexity of the algorithm.

Memory requirements. For $N = 1000$ and $\varepsilon = 10^{-7}$ the values of the elements of the sparse "matrices of influence" will occupy some 21 GB memory (see Table 1). With additional 12 GB for the indexes of the non-zero elements we arrive at 33 GB of memory for storage of these matrices. This fact made us decide to save the "matrices of influence" in pieces on the hard disk. Then the operations in (4.2)–(4.5) are executed by reading one piece at a time from HD, performing the multiplication and clearing the matrix piece from the memory before reading a new piece. In this way the execution time for 20 iterations is comparable to the time necessary to compute matrix element values in (4.1) and to save them on HD (see Table 2 below).

Each of the other input, work, and output variables as F, old and new g (i.e. g_k and g_{k+1}), spherical coordinates of the irregular sample points and the polynomial values requires $O(N^2)$ memory. In view of the small number of such variables this is easily manageable for N in the range of several thousand.

Optimal choice of needlet parameter τ. For $M = \lceil(2+\tau)N\rceil$, $K = \lceil M/2\rceil$, $L = M$ we have:

- The number of nodes in $\mathcal{X}_0$ is proportional to M^2.
- The average number of nodes from $\mathcal{X}_0$ in a δ neighborhood is proportional to $\delta^2 M^2$.

Hence, both the size of the "matrices of influence" and the number of operation in (4.2)–(4.5) for a single iteration step are proportional to $\delta^2 M^4$. Using (2.13) we get $\delta^2 M^4 = O((2+\tau)^4\tau^{-2}N^2)$ and the minimal value of the last expression is attained for $\tau = 2$. Therefore, the best choice of the needlet parameter τ relative to memory usage as well as speed is $\tau = 2$.

5. Numerical examples

5.1. Reconstruction

We have implemented our reconstruction algorithm in a MATLAB R2012b code and have extensively tested it on a 2.4 GHz PC, CPU Intel Core i7 with 16 GB of RAM. The code does not relay on variable precision arithmetic.

For irregular points we have taken the HEALPix pixel centers and their rotations on the sphere.

The optimal speed and memory requirements were achieved for $\tau = 2$ according to the theory. Hence, we report in this subsection results only for this value of the cutoff parameter. In the latitude direction the quadrature is Gaussian.

Please cite this article in press as: K. Ivanov, P. Petrushev, Irregular sampling of band-limited functions on the sphere, Appl. Comput. Harmon. Anal. (2014), http://dx.doi.org/10.1016/j.acha.2014.05.001

Table 1
Size of the "influence matrices": number of points in $\mathcal{X}_0$ and average number of non-zero elements.

N	ε			
	10^{-5}	10^{-7}	10^{-9}	10^{-11}
250	384 728 × 270	396 300 × 494	408 016 × 786	419 836 × 1150
500	1 470 932 × 268	1 493 560 × 488	1 516 332 × 773	1 539 128 × 1127
1000	5 749 660 × 267	5 794 400 × 485	5 839 244 × 767	5 884 128 × 1117

Table 2
Execution times (in minutes) of the reconstruction algorithm.

	Degree N			
	250	500	1000	2000
Pre-computation part	6.2	23.0	92.7	363.5
Iterations part (20 iterations)	6.2	24.2	96.1	384.4
Total	12.4	47.2	188.8	747.9

The dimensions of the "influence martices", i.e. the number of points in $\mathcal{X}_0$ and the average number of non-zero elements in (4.1), are displayed in Table 1 for $K = 2N$, $L = 4N$ and φ from (2.14)–(2.15).

For different irregular sampling sets Y the average number of non-zero elements may slightly vary. The number of points in $\mathcal{X}_0$ grows slowly when ε decreases due to the $\log \varepsilon$ enlargement of the adjacent sets $\mathcal{X}_1 \cap \mathcal{U}_2$ and $\mathcal{X}_2 \cap \mathcal{U}_1$.

The polynomial values were provided by several low and high degree polynomials. Among them were the polynomials G_N and $\widetilde{G}_N$ given by

$$G_N(\theta,\lambda) := \sum_{m=1}^{N} m^{-1/3} q_{m,N} P_{m,N}(\cos\theta)\sin(m\lambda) + \sum_{m=1}^{N-3} m^{-1/3} q_{m,N-3} P_{m,N-3}(\cos\theta)\sin(m\lambda),$$

$$\widetilde{G}_N(\theta,\lambda) := q_{0,N} P_{0,N}(\cos\theta) + 2\sum_{m=1}^{N} q_{m,N} P_{m,N}(\cos\theta)\cos(m\lambda),$$

where $P_{m,n}$ are the associated Legendre functions and the coefficients $q_{m,n}$ are selected so that they normalize to 1 in $L^2(\mathbb{S}^2, \frac{1}{4\pi} d\sigma)$ each spherical harmonic term.

The uniform norms of G_N and $\widetilde{G}_N$ for selected values of N are given in Tables 3 and 4, respectively. The global extrema of G_N and $\widetilde{G}_N$ are localized around the points $(\frac{\pi}{2}, \frac{\pi}{2})$ and $(\frac{\pi}{2}, \frac{3\pi}{2})$. We believe that the polynomials G_N and $\widetilde{G}_N$ are good for testing of our reconstruction algorithm since they have relatively large spherical harmonic coefficients and highly oscillatory behavior.

Table 2 contains the execution times of the *Pre-computation* and *Iterations* parts of the reconstruction algorithm. The *Pre-computation* time is the total of the times for execution of all steps of *Pre-computation* from Section 4 plus the saving time on HD. The *Iterations* time includes the execution times for all steps of *Iterations* plus the "matrices of influence" loading time from HD. The number of irregular sampling points is about 8 times larger than the number of regular points in $\mathcal{X}_0$, but their influence on the times reported below is minimal (apart from the number of iterations for achieving the target accuracy). The values of the other parameters are $\varepsilon = 10^{-7}$, $K = 2N$, $L = 4N$, and the number of iterations is 20.

We see that the execution times are proportional to N^2 according to the theory given in Section 4. The saving time is approximately 27% of the *Pre-computation* time, while the loading time is approximately 63% of the *Iterations* time.

The relative errors defined in (4.6) for $f = G_N$ and $f = \widetilde{G}_N$ at the regular points $\mathcal{X}_0$ are given in Tables 3 and 4, respectively. These errors are obtained from the algorithm from Section 4 and its modification described in Remark 3.2 with accuracy parameters $\varepsilon = 10^{-7}$ and $\varepsilon_2 = 10^{-8}$.

Please cite this article in press as: K. Ivanov, P. Petrushev, Irregular sampling of band-limited functions on the sphere, Appl. Comput. Harmon. Anal. (2014), http://dx.doi.org/10.1016/j.acha.2014.05.001

Table 3
Uniform norms and relative errors from (4.6) for G_N.

	Degree N			
	250	500	1000	2000
Uniform norm $\|G_N\|_\infty$	76.45	121.35	192.65	305.86
Algorithm from Section 4	8.4667e−09	7.8133e−09	5.7893e−09	5.8170e−09
Algorithm from Remark 3.2	9.6770e−09	1.1789e−08	9.2821e−09	9.5697e−09

Table 4
Uniform norms and relative errors from (4.6) for $\widetilde{G}_N$.

	Degree N			
	250	500	1000	2000
Uniform norm of $\|\widetilde{G}_N\|_\infty$	480.60	958.99	1915.4	3828.0
Algorithm from Section 4	5.6226e−09	5.6581e−09	5.4573e−09	5.3932e−09
Algorithm from Remark 3.2	6.5248e−09	6.6718e−09	6.0687e−09	6.0394e−09

As a rule the observed relative errors are 10 to 15 times smaller than the target relative accuracy ε_1! Our experiments also show that the relative errors from (4.7) at the sampling points Y are very close to the respective errors at the regular points $\mathcal{X}_0$.

5.2. Norms of operators

The operator norms in this subsection are $\infty \to \infty$ norms. The norm of the integral needlet operator (2.5) is given by

$$\|\check{\Phi}_N\| = \sup_{x\in\mathbb{S}^2} \frac{1}{4\pi} \int_{\mathbb{S}^2} \left|\mathcal{K}_N(x\cdot y)\right| d\sigma(y) = \frac{1}{2}\int_{-1}^{1} \left|\mathcal{K}_N(t)\right| dt. \tag{5.1}$$

For φ from (2.14)–(2.15) and for various τ and ε the numerical values of the norm from (5.1) for $N = 40$, $N = 400$, $N = 4000$ are displayed in Table 5.

As Table 5 shows the norm practically does not depend on the degree N. This fact is in compliance with the theory which states that these norms have majorants, which are independent of N. The slight decrease of the norm with N is predictable and is due to the increased smoothness of the kernel $\mathcal{K}_N$. The variations of the norm with τ and ε are due to the different functions φ defined in (2.14)–(2.15).

Table 5
Numerical evaluation of norm from (5.1).

τ	N	ε			
		10^{-5}	10^{-7}	10^{-9}	10^{-11}
1	40	3.1364	3.4067	3.6306	3.8230
	400	3.1280	3.3996	3.6251	3.8194
	4000	3.1267	3.3982	3.6236	3.8179
2	40	2.4559	2.6774	2.8613	3.0197
	400	2.4487	2.6700	2.8538	3.0123
	4000	2.4478	2.6691	2.8529	3.0114
3	40	2.1905	2.3927	2.5606	2.7054
	400	2.1849	2.3867	2.5545	2.6991
	4000	2.1842	2.3861	2.5538	2.6984
4	40	2.0510	2.2421	2.4010	2.5380
	400	2.0465	2.2373	2.3960	2.5328
	4000	2.0460	2.2368	2.3954	2.5323

Please cite this article in press as: K. Ivanov, P. Petrushev, Irregular sampling of band-limited functions on the sphere, Appl. Comput. Harmon. Anal. (2014), http://dx.doi.org/10.1016/j.acha.2014.05.001

Table 6
Numerical evaluation of $\|\Phi_N\|$ for $\mathcal{X} = \mathcal{X}^{(3)}$.

τ	ε			
	10^{-5}	10^{-7}	10^{-9}	10^{-11}
1	4.2324	4.6610	5.0166	5.3227
2	3.1562	3.5077	3.7990	4.0497
3	2.7355	3.0577	3.3245	3.5540
4	2.5137	2.8193	3.0724	3.2901

Table 7
Numerical evaluation of $\|\Phi_{N,\delta} \cdot \mathbb{1}_{\mathcal{U}_1} + \tilde{\Phi}_{N,\delta} \cdot \mathbb{1}_{\mathcal{U}_2}\|$ for $\mathcal{X} = \mathcal{X}^{(3)}$.

τ	ε			
	10^{-5}	10^{-7}	10^{-9}	10^{-11}
1	3.7265	4.0423	4.3022	4.5245
2	2.9159	3.1833	3.4026	3.5898
3	2.5899	2.8396	3.0438	3.2178
4	2.4152	2.6549	2.8507	3.0174

The norms of the discrete operators Φ_N and $\Phi_{N,\delta}$ are given by

$$\|\Phi_N\| = \sup_{x\in\mathbb{S}^2} \sum_{\xi\in\mathcal{X}} w_\xi \big|\Phi_N(x\cdot\xi)\big| \tag{5.2}$$

and

$$\|\Phi_{N,\delta}\| = \sup_{x\in\mathbb{S}^2} \sum_{\substack{\xi\in\mathcal{X}\\ \rho(x,\,\xi)\le\delta}} w_\xi \big|\Phi_N(x\cdot\xi)\big|. \tag{5.3}$$

Let us recall that due to (2.10) the two norms are quite close, namely,

$$0 < \|\Phi_N\| - \|\Phi_{N,\delta}\| \le \varepsilon.$$

The norms in (5.2) and (5.3) depend on N, δ, φ, τ, ε, K, L, and the type of the regular nodes used. As in the case of the norm in (5.1) the relative variation of these norms with respect to N is less than one percent.

For $N = 500$ and for various τ and ε the numerical values of the norm from (5.2) are displayed in Table 6. The other parameters for the computations are: Gaussian quadrature with $K = 2\lceil(2+\tau)N/4\rceil$, $L = 2K$, and φ from (2.14)–(2.15).

In Theorem 3.2 and in the solution of Problem 3 from [7] instead of $\Phi_{N,\delta}$ we in fact use the operators $\Phi_{N,\delta} \cdot \mathbb{1}_{\mathcal{U}_1} + \tilde{\Phi}_{N,\delta} \cdot \mathbb{1}_{\mathcal{U}_2}$. Their norms are given by

$$\|\Phi_{N,\delta} \cdot \mathbb{1}_{\mathcal{U}_1} + \tilde{\Phi}_{N,\delta} \cdot \mathbb{1}_{\mathcal{U}_2}\| = \sup_{\substack{x\in\mathbb{S}^2\\ \pi/4\le\theta\le 3\pi/4}} \sum_{\substack{\xi\in\mathcal{X}\\ \rho(x,\xi)\le\delta}} w_\xi \big|\Phi_N(x\cdot\xi)\big|. \tag{5.4}$$

These norms are given in Table 7 for the same values of the parameters as in Table 6.

According to (5.3) and (5.4)

$$\|\Phi_{N,\delta} \cdot \mathbb{1}_{\mathcal{U}_1} + \tilde{\Phi}_{N,\delta} \cdot \mathbb{1}_{\mathcal{U}_2}\| \le \|\Phi_{N,\delta}\|. \tag{5.5}$$

For the nodes $\mathcal{X} = \mathcal{X}^{(3)}$ generated by the Gaussian quadrature one has strict inequality in (5.5) as evidenced by Tables 6 and 7. The reason for this is that the supremums in (5.2) and (5.3) are attained for x at one of the poles, while the supremum in (5.4) is attained for x at the equator.

Please cite this article in press as: K. Ivanov, P. Petrushev, Irregular sampling of band-limited functions on the sphere, Appl. Comput. Harmon. Anal. (2014), http://dx.doi.org/10.1016/j.acha.2014.05.001

For $\mathcal{X} = \mathcal{X}^{(1)}$ or $\mathcal{X} = \mathcal{X}^{(2)}$ all supremums above are attained for x's at the equator and, hence, in (5.5) we have an equality. For these types of nodes and minimal possible K and L the norm values are approximately in the middle between the norm in (5.1) given in Tables 5 and the norm in (5.4) given in Table 7. The main reason for the decrease of the norm is that the number of knots in latitude direction is doubled. The general rule is that for a fixed cutoff function φ whenever the nodes get denser then the norm becomes smaller and tends to the value given in Table 5. Note that the parameters K and L are optimized for speed, but not to minimize $\|\Phi_N\|$.

The results in this subsection show that the norms of our needlet-type operators are quite small, which in turn guarantees the stability of the described algorithms.

Acknowledgments

The authors would like to thank the referees for their constructive suggestions for improvements.

References

[1] F. Dai, Y. Xu, Approximation Theory and Harmonic Analysis on Spheres and Balls, Springer, New York, 2013.
[2] H. Feichtinger, K. Gröchenig, Irregular sampling theorems and series expansions of bandlimited functions, J. Math. Anal. Appl. 167 (1992) 530–556.
[3] H. Feichtinger, K. Gröchenig, Iterative reconstruction of multivariate band-limited functions from irregular sampling values, SIAM J. Math. Anal. 231 (1992) 244–261.
[4] H. Feichtinger, K. Gröchenig, Theory and practice of irregular sampling, in: J. Benedetto, M. Frazier (Eds.), Wavelets: Mathematics and Applications, in: Stud. Adv. Math., CRC, Boca Raton, FL, 1994, pp. 305–363.
[5] H. Feichtinger, K. Gröchenig, T. Strohmer, Efficient numerical methods in nonuniform sampling theory, Numer. Math. 69 (1995) 423–440.
[6] A. Glaser, X. Liu, V. Rokhlin, A fast algorithm for the calculation of the roots of special functions, SIAM J. Sci. Comput. 29 (2007) 1420–1438.
[7] K.G. Ivanov, P. Petrushev, Fast memory efficient evaluation of spherical polynomials at scattered points, Adv. Comput. Math. (2014), http://dx.doi.org/10.1007/s10444-014-9354-3, to appear.
[8] J. Keiner, S. Kunis, D. Potts, Efficient reconstruction of functions on the sphere from scattered data, J. Fourier Anal. Appl. 13 (2007) 435–458.
[9] J. Keiner, A. Vollrath, A new algorithm for the nonequispaced fast Fourier transform on the rotation group, SIAM J. Sci. Comput. 34 (5) (2012) A2599–A2624.
[10] S. Kunis, D. Potts, Fast spherical Fourier algorithms, J. Comput. Appl. Math. 161 (2003) 75–98.
[11] S. Kunis, D. Potts, Stability results for scattered data interpolation by trigonometric polynomials, SIAM J. Sci. Comput. 29 (2007) 1403–1419.
[12] H.N. Mhaskar, F.J. Narcowich, J.W. Ward, Spherical Marcinkiewicz–Zygmund inequalities and positive quadrature, Math. Comp. 70 (235) (2001) 1113–1130.
[13] F. Narcowich, P. Petrushev, J. Ward, Localized tight frames on spheres, SIAM J. Math. Anal. 38 (2006) 574–594.
[14] F. Narcowich, P. Petrushev, J. Ward, Decomposition of Besov and Triebel–Lizorkin spaces on the sphere, J. Funct. Anal. 238 (2006) 530–564.
[15] L.N. Trefethen, et al., The Chebfun Development Team, Chebfun Version 4.2, http://www.maths.ox.ac.uk/chebfun/, 2011.

Please cite this article in press as: K. Ivanov, P. Petrushev, Irregular sampling of band-limited functions on the sphere, Appl. Comput. Harmon. Anal. (2014), http://dx.doi.org/10.1016/j.acha.2014.05.001